Electronic Supplementary Material (ESI) for Dalton Transactions.

Supporting Information

Late-stage derivatization of a $(B,O)_2$-doped perylene

Omar Ouadoudi, Tanja Kaehler, Enes Görkem Çevik, Michael Bolte, Berthold Stöger, Alexander Virovets,
Hans-Wolfram Lerner and Matthias Wagner

Table of contents:

1. General experimental procedures S3
2. Bromination of **1** S4
    2.1. Synthesis of **2** using Br_2 ..... S4
    2.2. Synthesis of **2** using $CuBr_2$ S6
    2.3. Synthesis of **3** S6
    2.4. Synthesis of **4** S6
3. Synthesis of **5** and **6** by Stille-type coupling S7
    3.1. Synthesis of **5** S7
    3.2. Synthesis of **6** S8
4. Plots of ^1H, $^{13}C\{^1H\}$, and ^{11}B NMR spectra of **5** and **6** S9
5. Attempted Miyaura borylation of **2** S13
6. Photophysical and electrochemical data S15
    6.1. UV/Vis absorption and emission spectra S16
    6.2. Plots of cyclic voltammograms S18
7. X-ray crystal structure analyses S19
8. References S26

1. General experimental procedures

If not stated otherwise, all reactions and manipulations were carried out under an atmosphere of dry N_2 using Schlenk techniques or in an inert-atmosphere glovebox. Toluene was distilled from Na/benzophenone and degassed by three freeze-pump-thaw cycles prior to use. CH_2Cl_2 and NEt_3 were distilled from CaH_2. CD_2Cl_2, $CDCl_3$, and *t*BuOH were stored over molecular sieves (3 Å). The starting materials *n*$Bu_3SnC{\equiv}CMe$,[S1] *n*$Bu_3SnC{\equiv}C(C_6H_4$*t*Bu),[S2] and 2,8-dimethyl-1,7-dioxa-6b,12b-diboraperylene (**1**)[S3] were prepared according to literature procedures. $AlBr_3$ (*Acros Organics*), Br_2 (*Acros Organics*), $CuBr_2$ (*Sigma Aldrich*), [Ni(dppp)Cl_2](*Sigma Aldrich*), HBpin (*Sigma Aldrich*), and [Pd(P*t*$Bu_3)_2$] (*Alfa Aesar*) were used as received. Reaction mixtures were heated by using an oil bath.

NMR spectra were recorded at 298 K using the following spectrometers: Bruker Avance-300 or Avance-500. Chemical shift values are referenced to (residual) solvent signals ($^1H/^{13}C\{^1H\}$; CD_2Cl_2: δ = 5.32/n.a. ppm, $CDCl_3$: δ = 7.26/77.16 ppm)[S4] or external $BF_3{\cdot}Et_2O$ (^{11}B: 0.00 ppm). Abbreviations: s = singlet, d = doublet, dd = doublet of doublets, m = multiplet, br. = broad, n.o. = not observed. Resonances of carbon atoms attached to boron atoms were typically broadened and sometimes not observed due to the quadrupolar relaxation of boron. Boron resonances of triarylborane compounds are typically very broad ($h_{1/2}$ > 1100 Hz) and were observed only in highly concentrated samples. Resonance assignments were aided by ^{H,H}COSY, ^{H,C}HSQC, and ^{H,C}HMBC spectra. **Note:** The numbering scheme employed for the assignment of NMR resonances deviates from the IUPAC nomenclature. For simplicity, only chemically inequivalent positions are numbered; for better comparability, identical fragments have always been given the same numbers.

UV/Vis absorption spectra were recorded at room temperature using a *Varian* Cary 50 Scan or a *Varian* Cary 60 Scan UV/Vis spectrophotometer. Photoluminescence (PL) spectra were recorded at room temperature using a *Jasco* FP-8300 spectrofluorometer equipped with a calibrated *Jasco* ILF-835 100 mm diameter integrating sphere and analyzed using the *Jasco* FWQE-880 software. For PL quantum yield (Φ_{PL}) measurements, each sample was carefully degassed with argon using an injection needle and a septum-capped cuvette. Under these conditions, the Φ_{PL} of the fluorescence standard 9,10-diphenylanthracene was determined as 97% (lit.: 97%).[S5,S6] For all Φ_{PL} measurements, at least three samples of different concentrations were used (range between 10^{-5} and 10^{-7} mol L^{-1}). Due to self-absorption, slightly lower Φ_{PL} values were observed at higher concentrations. This effect was corrected by applying a method reported by *Bardeen et al.*, which slightly improved the Φ_{PL} values (2% at most).[S7] Cyclic voltammetry (CV) measurements were performed in a glovebox at room temperature in a one-chamber, three-electrode cell using an *EG&G* Princeton Applied Research 263A potentiostat. A platinum-disk electrode (2.00 mm diameter) was used as the working electrode with a platinum-wire counter electrode and a silver-wire reference electrode, which was coated with AgCl by immersion into HCl/HNO_3 (3:1). Prior to measurements, the solvents CH_2Cl_2 and THF were dried with CaH_2 and NaK, respectively, and degassed by three freeze-pump-thaw cycles. [*n*Bu_4N][PF_6] (*Sigma Aldrich*; used as received) was employed as the supporting electrolyte (0.1 mol L^{-1}). All potential values were referenced against the FcH/FcH^+ redox couple (FcH = ferrocene; $E_{1/2}$ = 0 V). Scan rates were varied between 100 and 400 mV s^{-1}. High-resolution mass spectra were measured in positive mode using a *Thermo Fisher Scientific* MALDI LTQ Orbitrap XL spectrometer and 2,5-dihydroxybenzoic acid or α-cyano-4-hydroxycinnamic acid as the matrix.

2. Bromination of 1

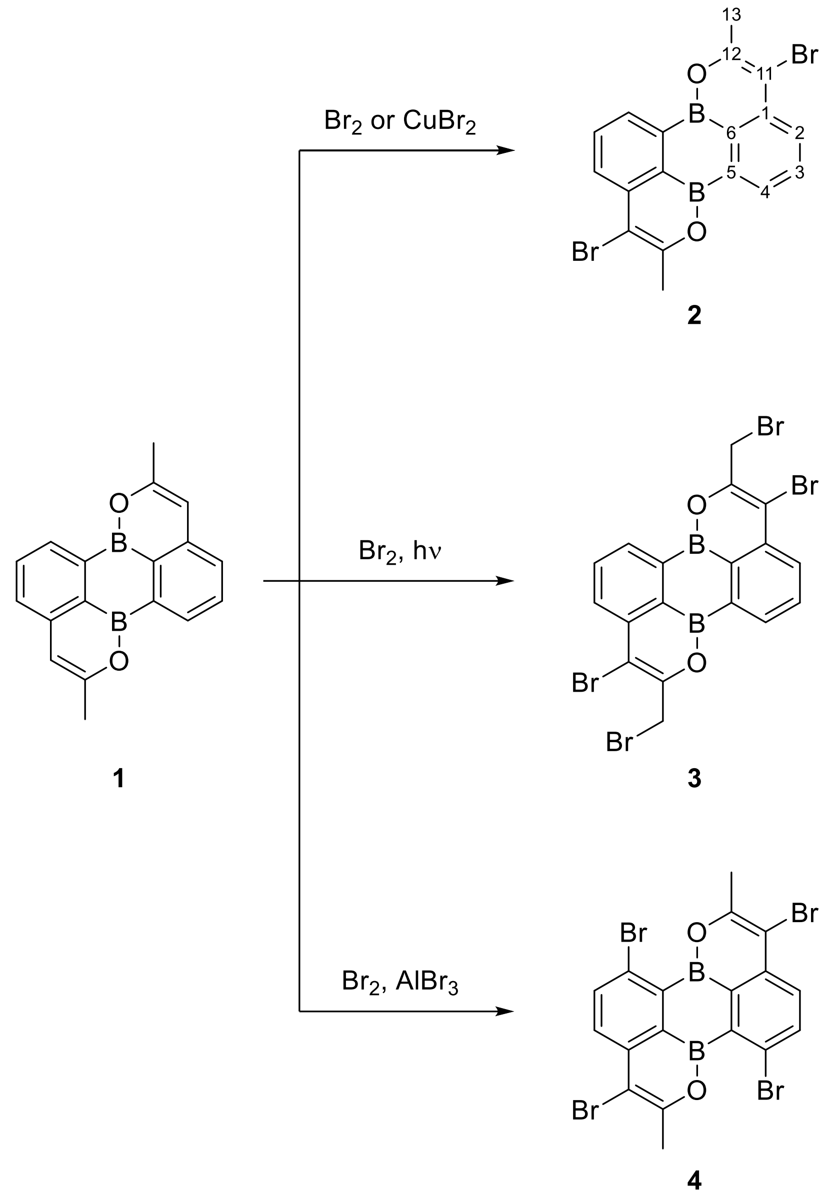

2.1. Synthesis of 2 using Br$_2$

A Schlenk flask was wrapped in aluminum foil, charged with **1** (0.020 g, 0.070 mmol), and evacuated for 0.5 h. The solid was dissolved in CH_2Cl_2 (10 mL) and neat Br_2 (0.04 mL, 0.12 g, 0.75 mmol) was added in the dark. The reaction mixture was stirred in the dark at room temperature for 2.5 h. A yellow precipitate formed, which was isolated by filtration and washed with CH_2Cl_2 (2 × 2 mL). **2** was obtained as a yellow solid. Yield: 0.022 g (0.050 mmol, 71%).

The solubility of **2** in all common solvents is low; it was, however, possible to record ^{1}H and ^{11}B NMR spectra in $CDCl_3$ at room temperature, albeit with poor signal-to-noise-ratios. Yellow platelets suitable for X-ray analysis were grown by recrystallization of **2** from boiling THF.

Further proof for the proposed molecular structure of **2** was gained by derivatization (see the dialkynyl derivative **5**, which has been fully characterized).

^{1}H NMR (500.2 MHz, $CDCl_3$): δ = 8.15 (dd, ^3J(H,H) = 7.1 Hz, ^4J(H,H) = 1.0 Hz, 2H; H-2 or H-4), 8.01 (dd, ^3J(H,H) = 7.9 Hz, ^4J(H,H) = 1.0 Hz, 2H; H-2 or H-4), 7.80 (dd, ^3J(H,H) = 7.9 Hz, ^3J(H,H) = 7.1 Hz, 2H; H-3), 2.71 (s, 6H; H-13).

^{11}B NMR (96.3 MHz, $CDCl_3$): δ = 39 ($h_{1/2} \approx$ 800 Hz).

HRMS: Calculated m/z for $[C_{18}H_{12}B_2Br_2O_2]^+$: 441.93642 found: 441.93583

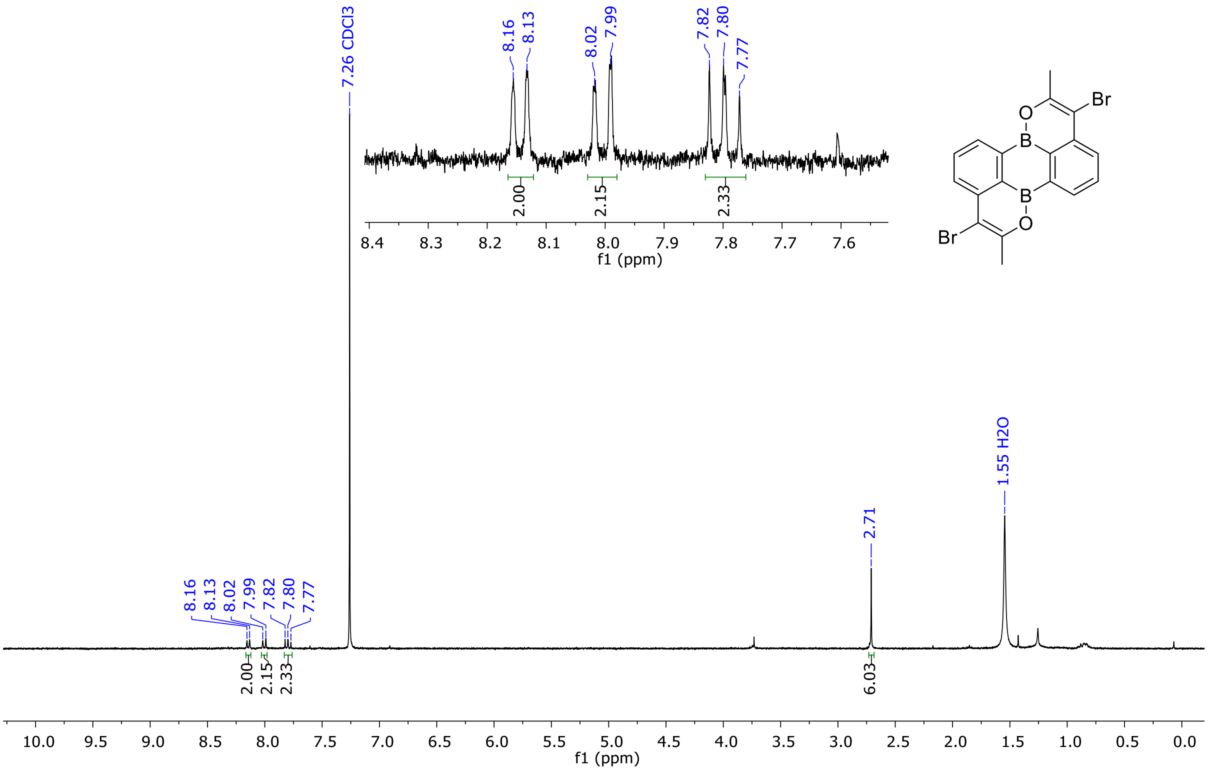

Figure S1: ^{1}H NMR spectrum of the precipitated **2** ($CDCl_3$, 500.2 MHz).

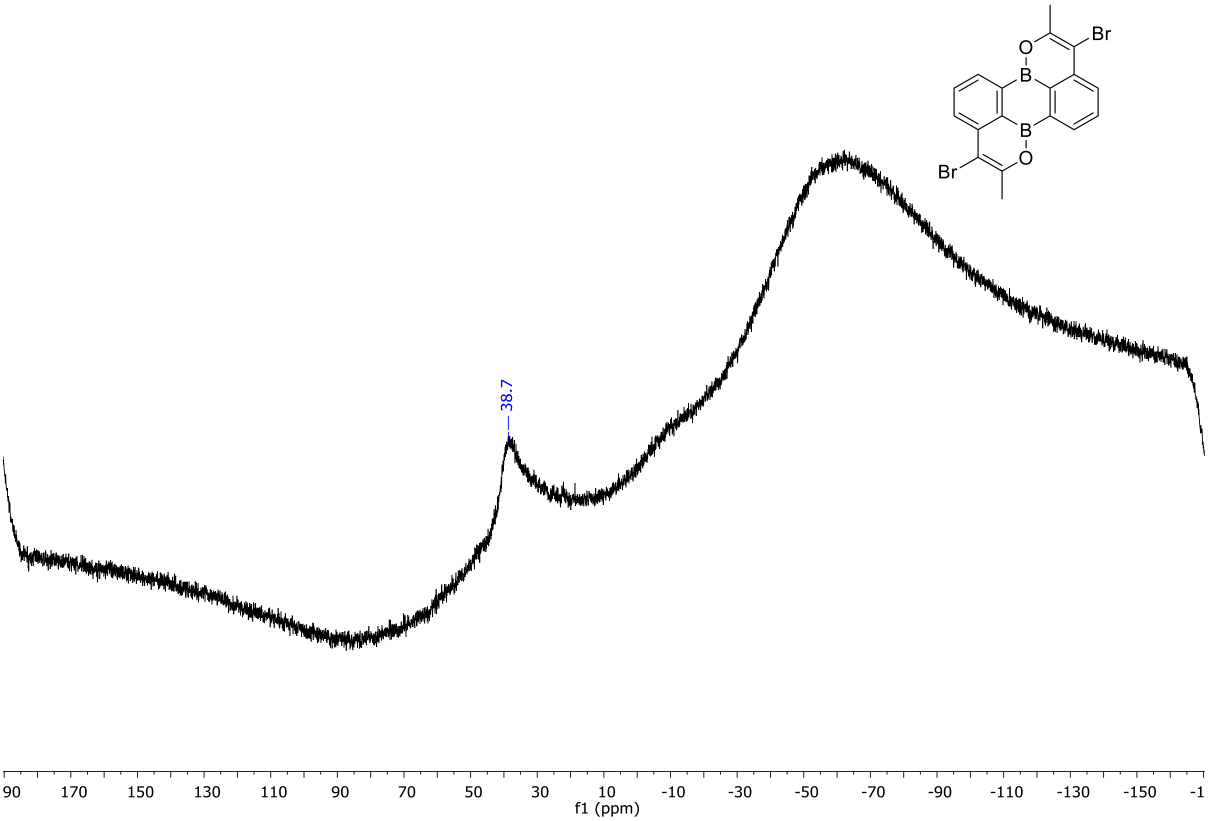

Figure S2: ^{11}B NMR spectrum of the precipitated **2** ($CDCl_3$, 96.3 MHz).

2.2. Synthesis of 2 using $CuBr_2$

A Schlenk flask was charged with **1** (0.020 g, 0.070 mmol) and $CuBr_2$ (0.094 g, 0.42 mmol) and evacuated for 0.5 h. The solids were suspended in *t*BuOH (10 mL). The suspension was stirred at 35 °C for 3 d and then evaporated to dryness. The solid residue was taken up in $CHCl_3$ and filtered over a short plug of silica gel with $CHCl_3$ as eluent. All volatiles were removed from the filtrate under reduced pressure and the crude product was washed with CH_2Cl_2 (2 × 1 mL). **2** was obtained as a yellow solid. Yield: 0.020 g (0.045 mmol, 64%).

2.3. Synthesis of 3

A Schlenk flask was charged with **1** (0.020 g, 0.070 mmol) and evacuated for 0.5 h. The solid was dissolved in CH_2Cl_2 (30 mL), and Br_2 (0.04 mL, 0.12 g, 0.75 mmol) was added. The reaction mixture was irradiated for 2 h with a conventional desktop lamp (medium-pressure Hg-vapor lamp, 9 W). The resulting yellow precipitate was isolated by filtration and washed with CH_2Cl_2 (2 × 1 mL). **3** was obtained as a yellow solid. Yield: 0.030 g (0.050 mmol, 71%).

The solubility of **3** in all common solvents is too low to record NMR spectra. Yellow needles suitable for X-ray analysis were grown by recrystallization of **3** from boiling C_6H_6.

2.4. Synthesis of 4

A Schlenk flask was wrapped in aluminum foil and charged with $AlBr_3$ (0.019 g, 0.071 mmol), Br_2 (0.04 mL, 0.12 g, 0.75 mmol), and CH_2Cl_2 (20 mL). The red solution was cooled to 0 °C and **1** (0.020 g, 0.070 mmol) was added in the dark. The reaction mixture was gradually warmed to room temperature and stirred for 17 h under strict exclusion of light. A yellow precipitate formed, which was isolated by filtration and washed with CH_2Cl_2 (2 × 1 mL) and H_2O (2 × 1 mL). **4** was obtained as a yellow solid. Yield: 0.022 g (0.037 mmol, 52%).

The solubility of **4** in all common solvents is too low to record NMR spectra. Yellow needles suitable for X-ray analysis were grown by recrystallization of **4** from boiling C_6H_6.

Further proof for the proposed molecular structure of **4** was gained by derivatization (see the tetraalkynyl derivative **6**).

Note: When the amount of $AlBr_3$ was increased, a significant decrease in yield was noticed. If more than 2 equiv. of $AlBr_3$ were used, the reaction solution turned black and no formation of **4** was observed. Most importantly, depending on the quality of the $AlBr_3$ employed, the yield ranged from 40% to 80% (vessel freshly opened immediately after it was received from the supplier); the 52% yield mentioned above is the average value over 10 runs.

HRMS: Calculated m/z for $[C_{18}H_{10}B_2Br_4O_2]^+$: 599.75540 found: 599.75426

3. Synthesis of 5 and 6 by Stille-type coupling

3.1. Synthesis of 5

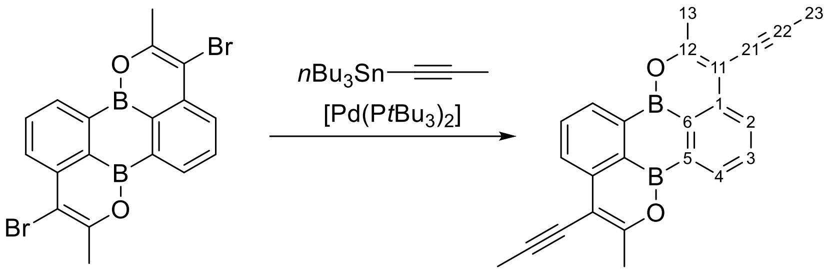

2 **5**

A Schlenk tube was charged with **2** (0.022 g, 0.050 mmol) and [Pd(P*t*Bu$_3$)$_2$] (0.003 g, 0.006 mmol) and kept under a dynamic vacuum for 0.5 h. The solids were suspended in toluene (20 mL) and neat *n*Bu$_3$SnC≡CMe (0.066 g, 0.200 mmol) was added. The reaction mixture was heated to 80 °C for 20 h, allowed to cool to room temperature, and evaporated to dryness. The solid residue was dissolved in CHCl$_3$ and filtered over a short plug of silica gel with CHCl$_3$ as eluent. All volatiles were removed from the filtrate under reduced pressure and the crude product was washed with *n*-hexane (3 × 2 mL). **5** was obtained as a yellow solid. Yield: 0.015 g (0.042 mmol, 84%). Single crystals were grown by slow evaporation of a solution of **5** in CHCl$_3$.

^{1}H NMR (500.2 MHz, CDCl$_3$): δ = 8.13 (dd, ^{3}J(H,H) = 7.1 Hz, ^{4}J(H,H) = 1.0 Hz, 2H; H-4), 8.02 (dd, ^{3}J(H,H) = 7.9 Hz, ^{4}J(H,H) = 1.0 Hz, 2H; H-2), 7.76 (dd, ^{3}J(H,H) = 7.9 Hz, ^{3}J(H,H) = 7.1 Hz, 2H; H-3), 2.66 (s, 6H; H-13), 2.21 (s, 6H; H-23)
^{13}C{^{1}H} NMR (125.8 MHz, CDCl$_3$): δ = 158.0 (C-12), 140.3 (C-1), 133.9* (br.; C-6), 132.9 (C-3), 130.4 (C-4), 127.7 (C-2), 104.6 (C-11), 92.1 (C-22), 74.8 (C-21), 21.1 (C-13), 4.8 (C-23), n.o. (C-5); (*) unequivocally detected only in the $^{\text{H,C}}$HMBC spectrum
^{11}B NMR (96.3 MHz, CDCl$_3$): δ = 37 ($h_{1/2} \approx$ 1350 Hz)
HRMS: Calculated *m*/*z* for $[C_{24}H_{18}B_2O_2]^+$: 360.14874, found: 360.14972
UV/Vis (CHCl$_3$): $\lambda_{\max}$ (ε) = 379 (11500), 396 (16300), 417 nm (12600 mol^{-1}dm^{3}cm^{-1})
Fluorescence (CHCl$_3$, λ_{ex} = 397 nm): $\lambda_{\max}$ = 441, 462, 500 (sh; resolved vibrational fine-structure) nm; Φ_{PL} = 51%
Cyclic voltammetry (THF, [*n*Bu$_4$N][PF$_6$] 0.1 M, 200 mV s^{-1}, vs. FcH/FcH$^+$): $E_{1/2}$ = –2.20 V
Melting point: 266 °C (decomposition)

3.2. Synthesis of 6

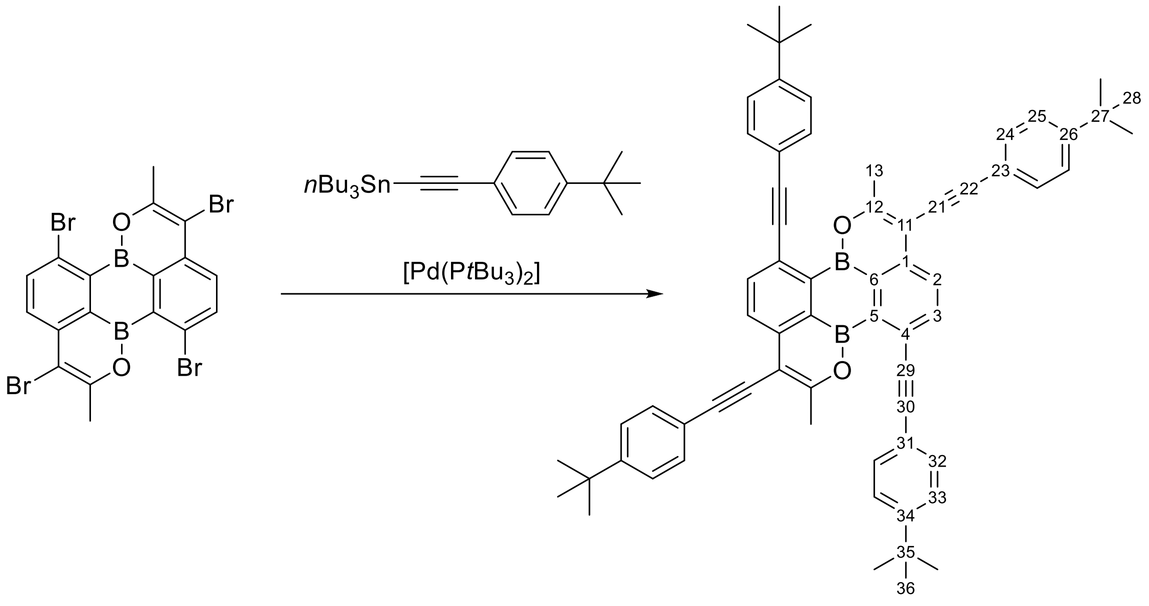

4 6

A Schlenk tube was charged with **4** (0.040 g, 0.067 mmol) and [Pd(P*t*Bu$_3$)$_2$] (0.006 g, 0.012 mmol) and kept under a dynamic vacuum for 0.5 h. The solids were suspended in toluene (80 mL) and neat *n*Bu$_3$SnC≡C(*p*-C$_6$H$_4$*t*Bu) (0.14 g, 0.31 mmol) was added. The reaction mixture was heated to 85 °C for 20 h, allowed to cool to room temperature, and evaporated to dryness. The solid residue was dissolved in CHCl$_3$ and filtered over a short plug of silica gel with CHCl$_3$ as eluent. All volatiles were removed from the filtrate under reduced pressure and the crude product was washed with MeCN (3 × 2 mL) and *n*-hexane (3 × 1 mL). **6** was obtained as a yellow solid. Yield: 0.038 g (0.042 mmol, 63%). Yellow needles suitable for X-ray analysis were grown by recrystallization of **6** from boiling C$_6$H$_6$.

The solubility of **6** in all common solvents is low; it was, however, possible to record ^{1}H NMR and ^{11}B NMR spectra in CD$_2$Cl$_2$ and CDCl$_3$ at room temperature.

^{1}H NMR (300.2 MHz, CD$_2$Cl$_2$): δ = 8.08 (d, ^3J(H,H) = 8.2 Hz, 2H; H-2 or H-3), 7.89 (d, ^3J(H,H) = 8.2 Hz, 2H; H-2 or H-3), 7.63–7.61 (m, 4H; H-24 or H-32), 7.57–7.54 (m, 4H; H-24 or H-32), 7.45–7.42 (m, 8H; H-25, H-33), 2.69 (s, 6H; H-13), 1.36 (s, 36H; H-28, H-36).

^{1}H NMR (300.2 MHz, CDCl$_3$): δ = 8.07 (d, ^3J(H,H) = 8.4 Hz, 2H; H-2 or H-3), 7.89 (d, ^3J(H,H) = 8.4 Hz, 2H; H-2 or H-3), 7.62–7.60 (m, 4H; H-24 or H-32), 7.56–7.53 (m, 4H; H-24 or H-32), 7.42–7.39 (m, 8H; H-25, H-33), 2.68 (s, 6H; H-13), 1.36 (s, 36H; H-28, H-36).

^{11}B NMR (96.3 MHz, CD$_2$Cl$_2$): δ = 45 ($h_{1/2} \approx$ 2200 Hz).

^{11}B NMR (96.3 MHz, CDCl$_3$): δ = 42 ($h_{1/2} \approx$ 1900 Hz).

HRMS: Calculated m/z for [C$_{66}$H$_{62}$B$_2$O$_2$]$^+$: 908.49304, found: 908.49327.

UV/Vis (CHCl$_3$): λ_{max} (ε) = 318 (80000), 401 (sh), 431 (16200), 452 nm (12700 mol^{-1}dm^{3}cm^{-1}).

Fluorescence (CHCl$_3$, λ_{ex} = 318 nm): λ_{max} = 481, 506, 559 (sh; resolved vibrational fine-structure) nm; Φ_{PL} = 34%.

Cyclic voltammetry (THF, [*n*Bu$_4$N][PF$_6$] 0.1 M, 200 mV s^{-1}, vs. FcH/FcH$^+$): $E_{1/2}$ = –2.00, –2.44 V.

Melting point: >255 °C (decomposition).

4. Plots of ^{1}H, $^{13}C\{^{1}H\}$, and ^{11}B NMR spectra of 5 and 6

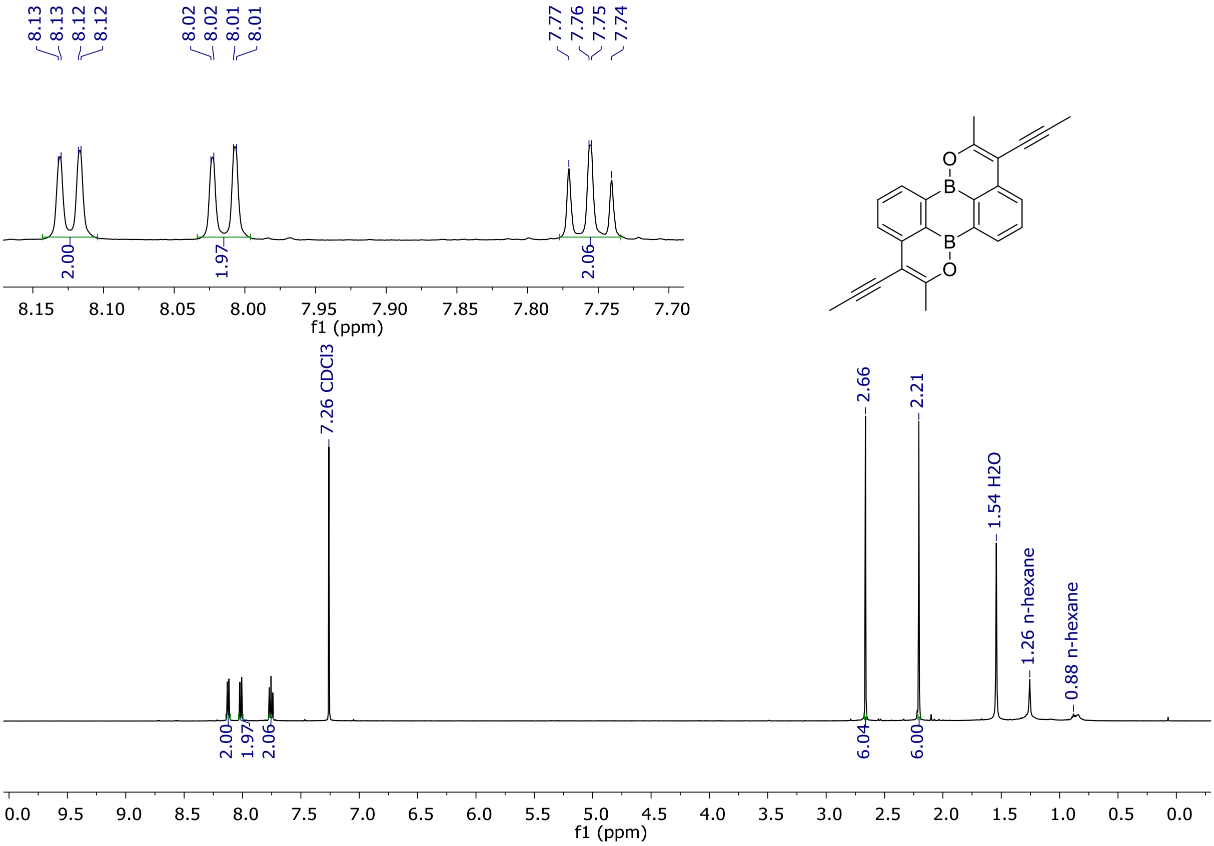

Figure S3: ^{1}H NMR spectrum of **5** ($CDCl_3$, 500.2 MHz).

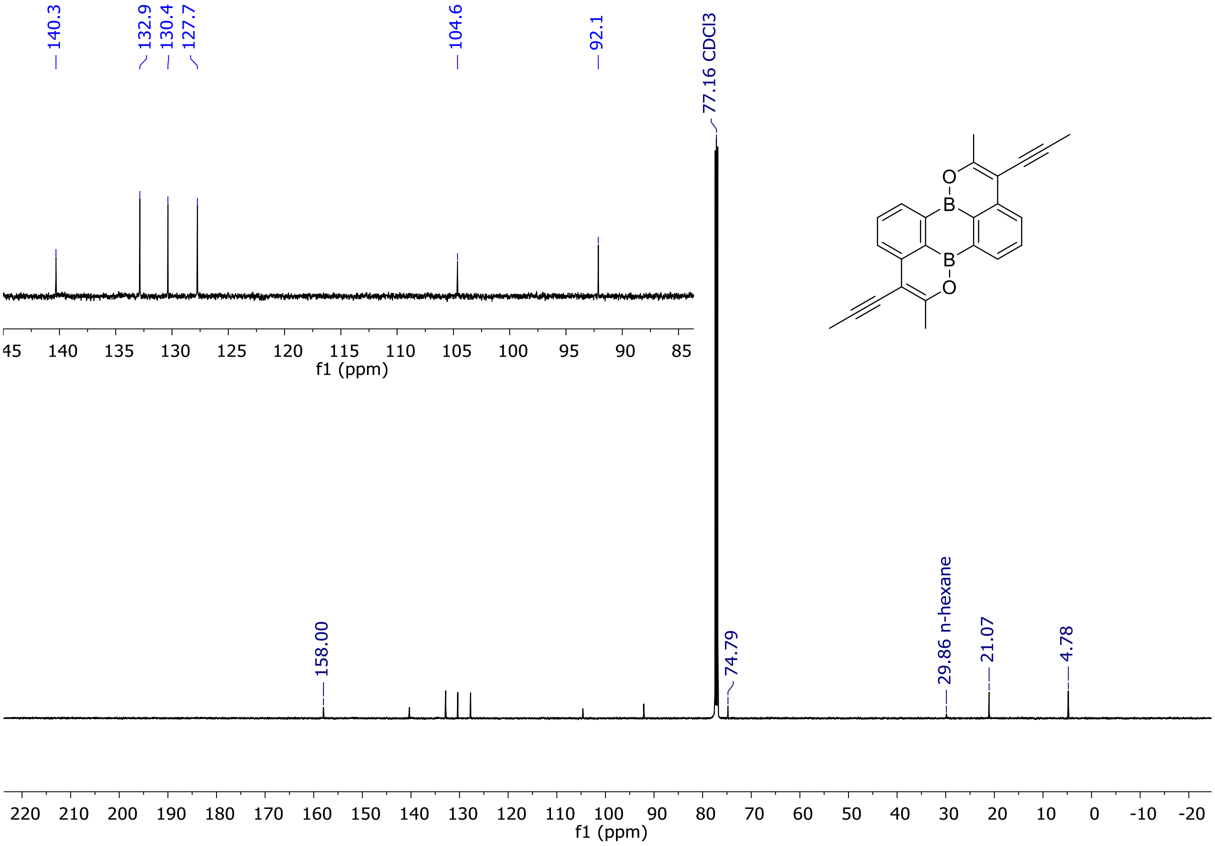

Figure S4: $^{13}C\{^{1}H\}$ NMR spectrum of **5** ($CDCl_3$, 125.8 MHz).

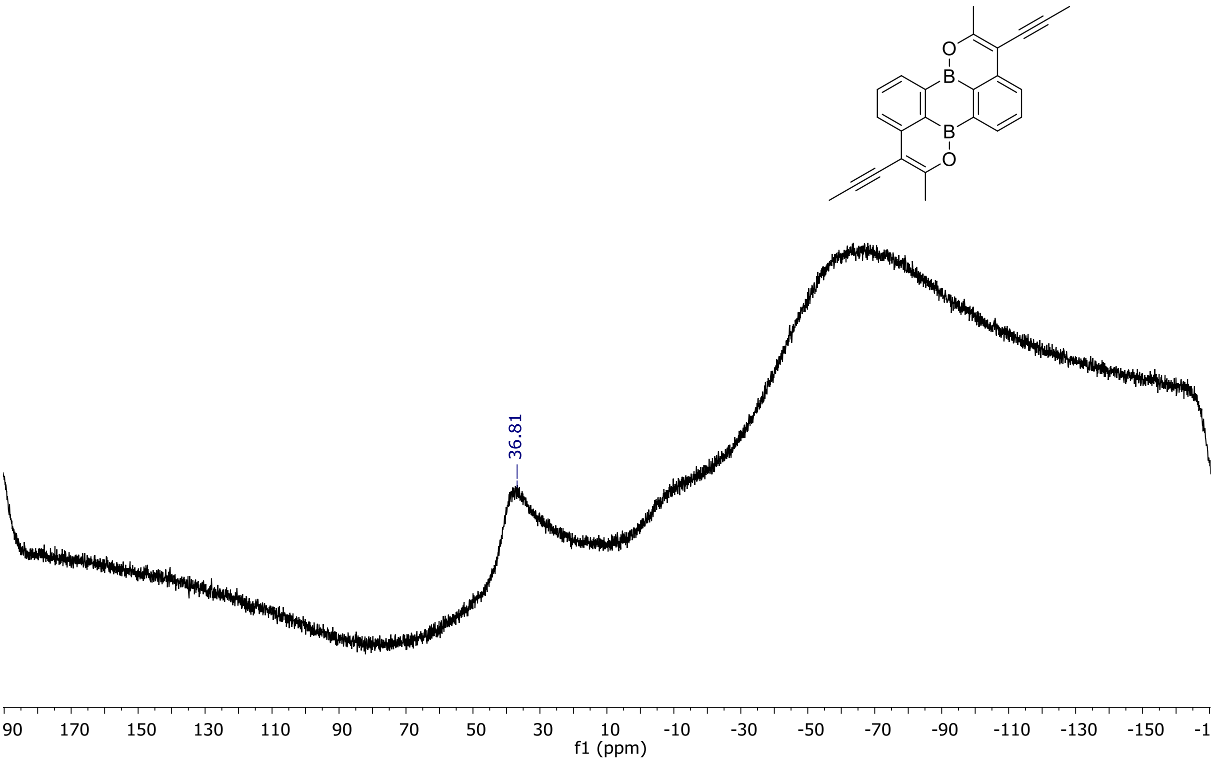

Figure S5: ^{11}B NMR spectrum of **5** ($CDCl_3$, 96.3 MHz).

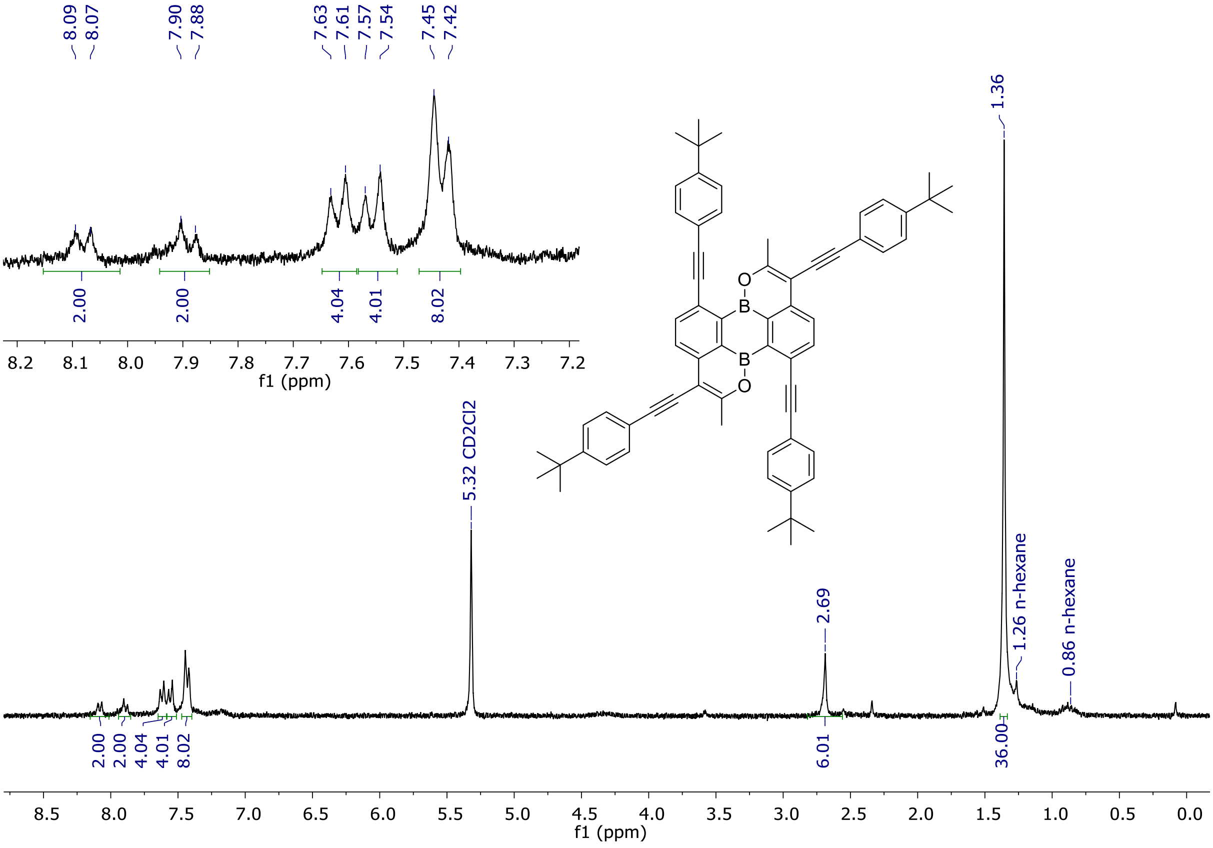

Figure S6: ^{1}H NMR spectrum of **6** (CD_2Cl_2, 300.2 MHz).

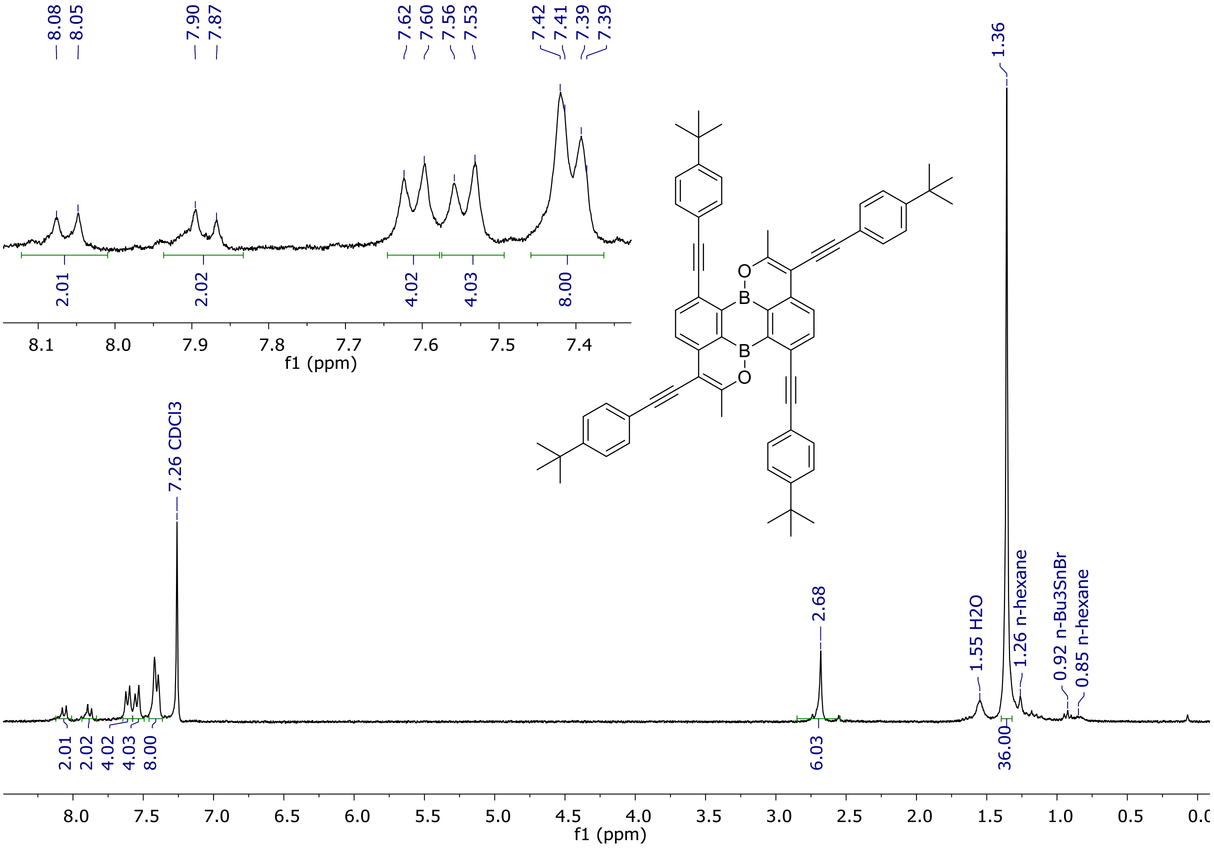

Figure S7: ^{1}H NMR spectrum of **6** ($CDCl_3$, 300.2 MHz).

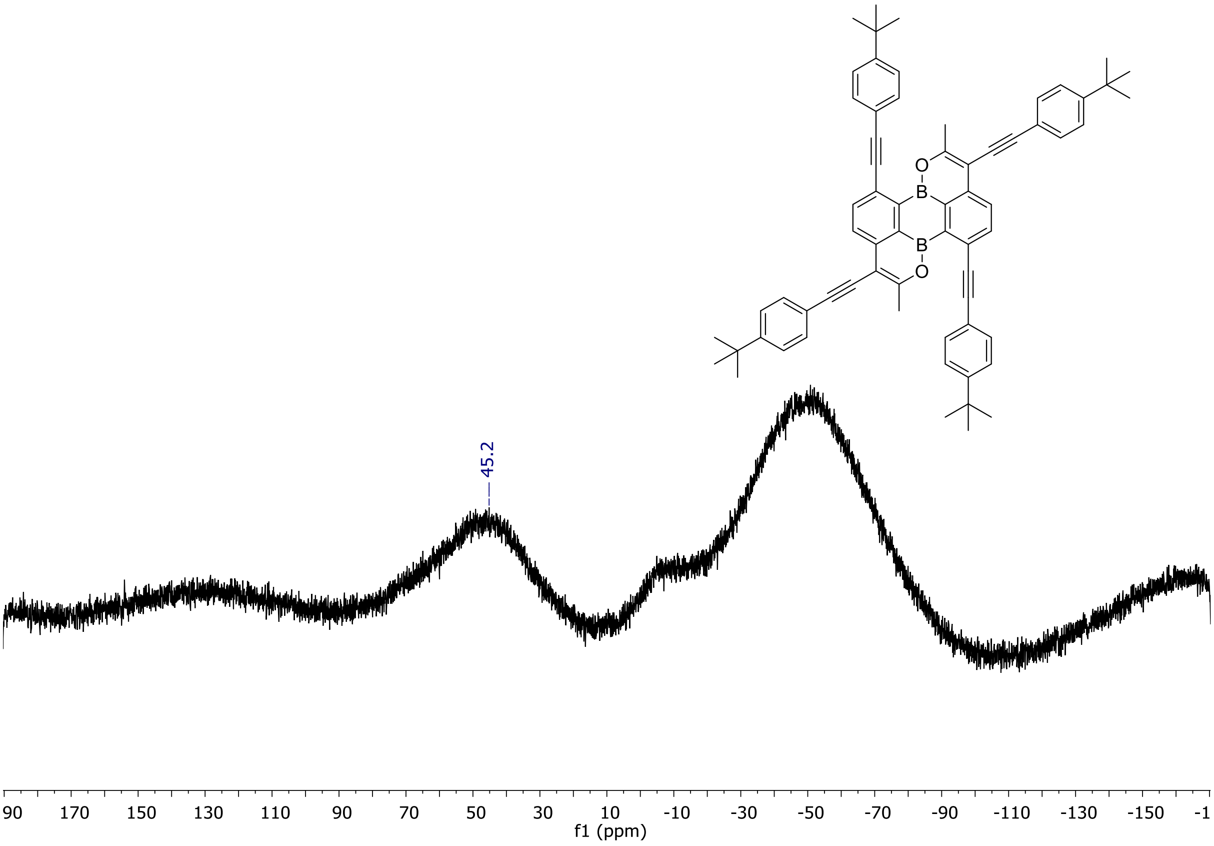

Figure S8: ^{11}B NMR spectrum of **6** (CD_2Cl_2, 96.3 MHz).

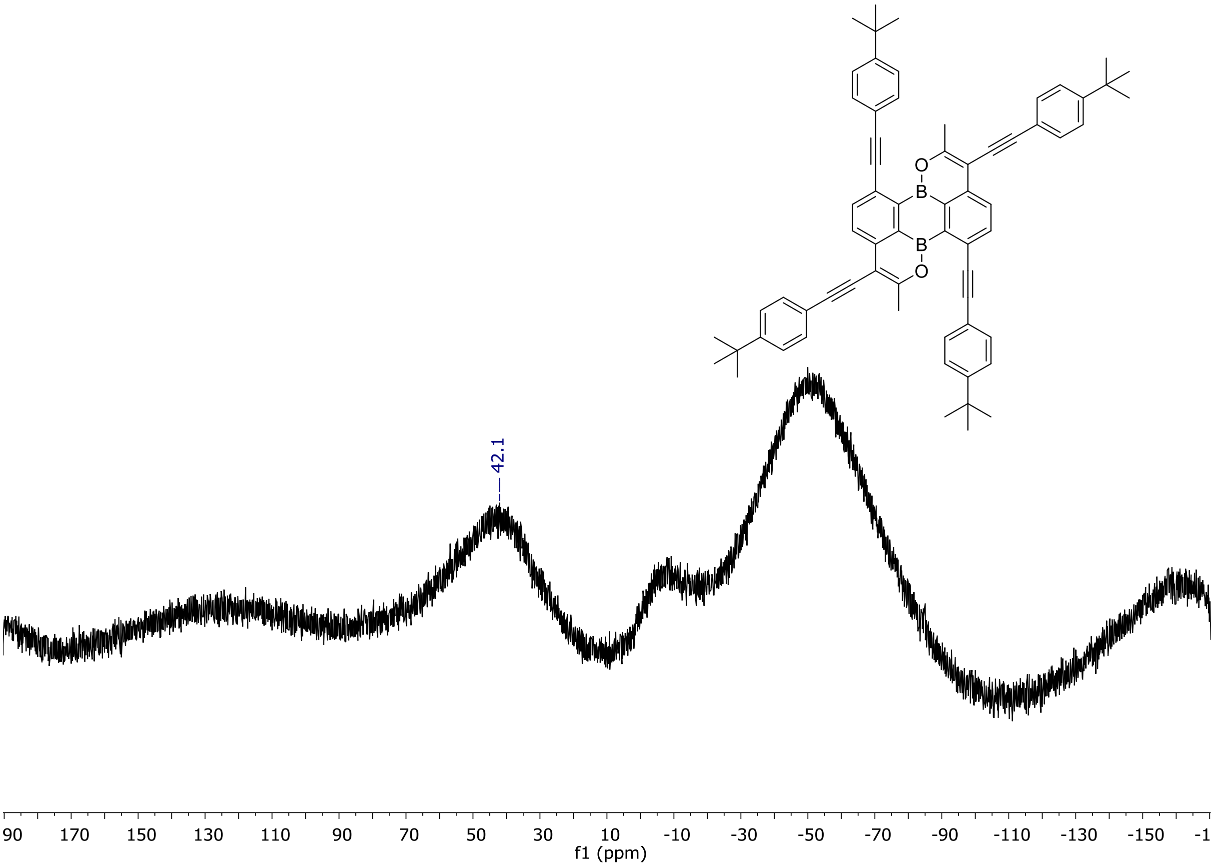

Figure S9: ^{11}B NMR spectrum of **6** ($CDCl_3$, 96.3 MHz).

5. Attempted Miyaura borylation of 2

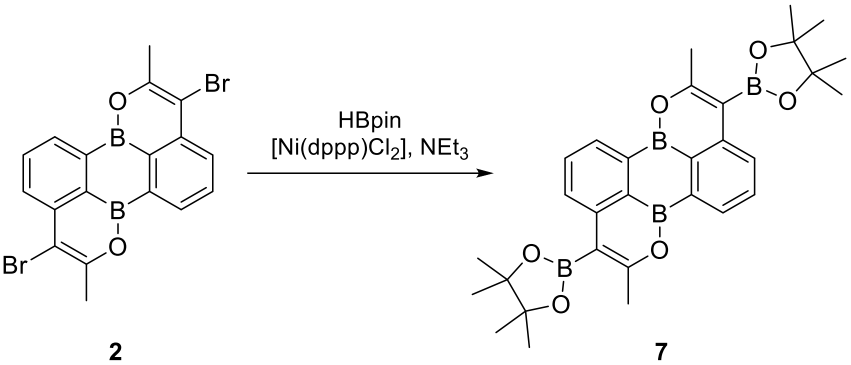

2 **7**

A microwave vial was charged with **2** (0.018 g, 0.041 mmol) and [Ni(dppp)Cl_2] (0.008 g, 0.015 mmol), evacuated for 0.5 h, and closed with a septum cap. After the addition of toluene (15 mL), NEt_3 (0.21 mL, 1.5 mmol), and HBpin (0.12 g, 0.94 mmol) the mixture was heated to 130 °C for 48 h under an N_2 atmosphere. The reaction mixture was cooled to room temperature and H_2O (10 mL) was added. The two liquid phases were separated, and the aqueous phase was extracted with $CHCl_3$ (2 × 10 mL). The combined organic phases were washed with H_2O (20 mL) and dried over $MgSO_4$. After filtration, all volatiles were removed from the filtrate under reduced pressure. The solid residue was washed with MeOH (2 × 2 mL) to give a yellow solid (0.009 g). According to the ^1H and ^{11}B NMR spectra, a mixture of the product **7** and the protodeborylated form **1** is present (Figure S10 and Figure S11).

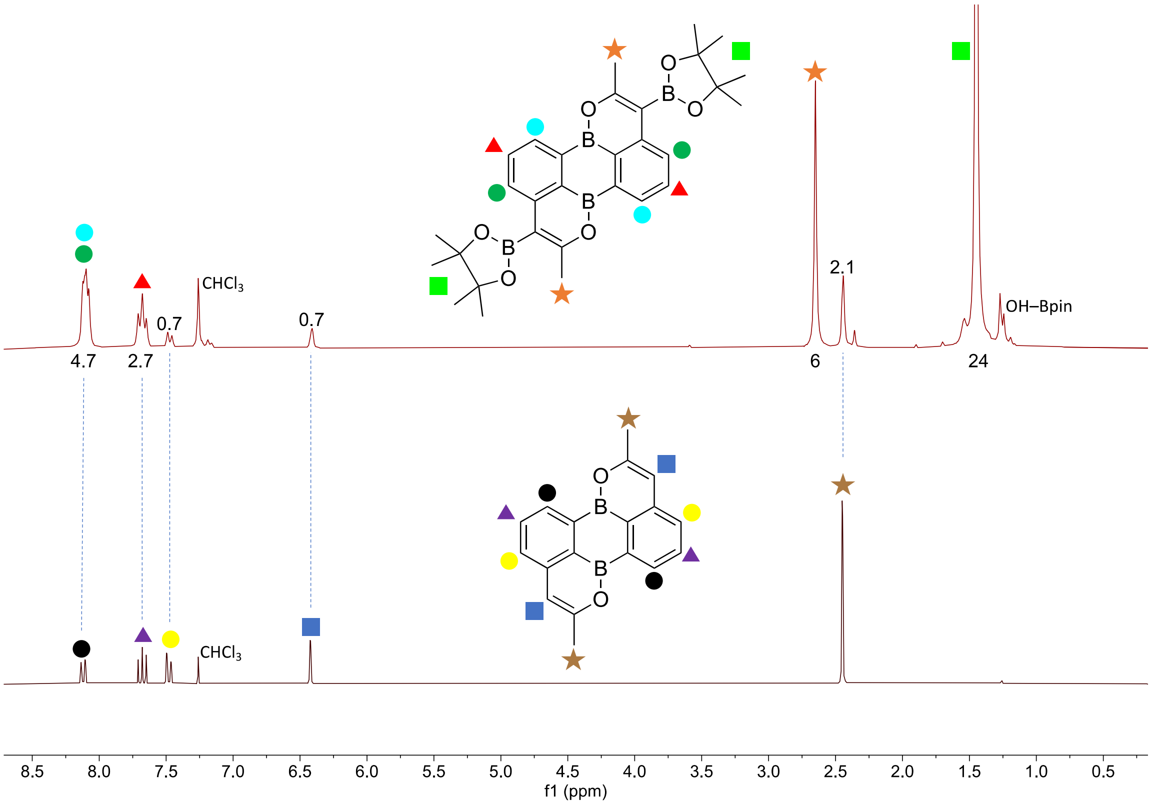

Figure S10: ^1H NMR spectrum of the mixture of **7** and **1** (top) in comparison with pure **1** (bottom; $CDCl_3$, 250.1 MHz).

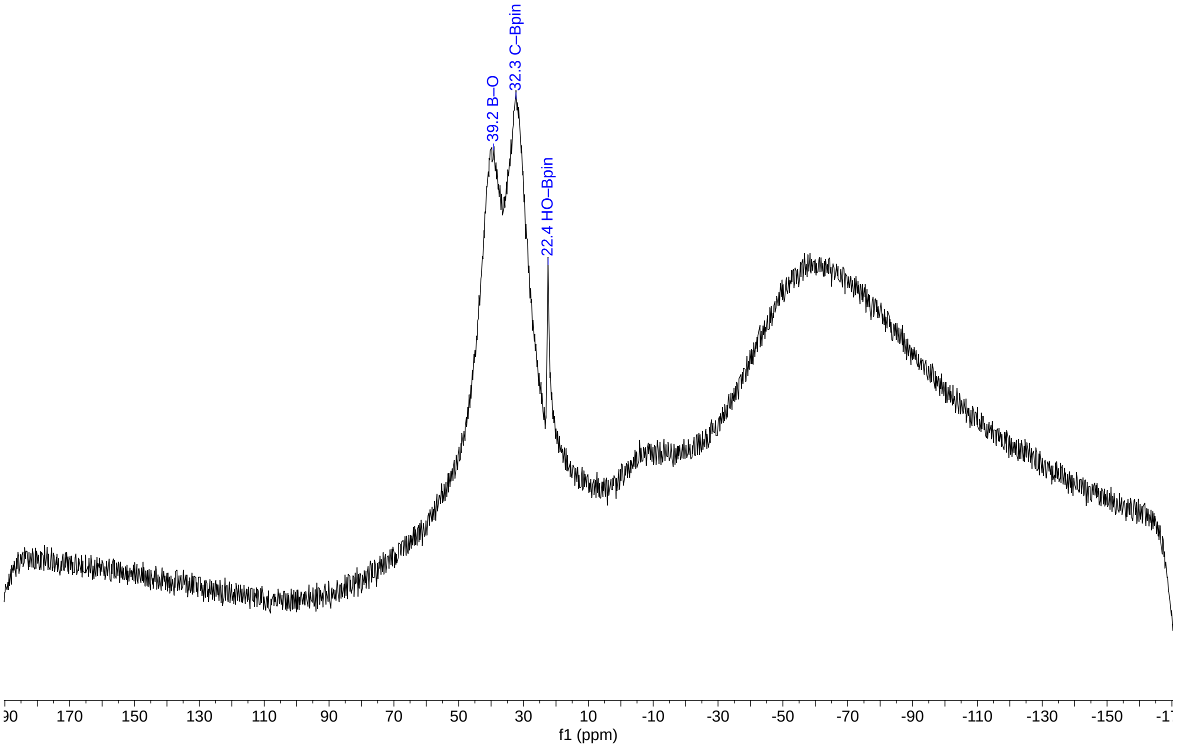

Figure S11: ^{11}B NMR spectrum of the mixture of **7** and **1** ($CDCl_3$, 96.3 MHz).

6. Photophysical and electrochemical data

Table S1: Photophysical and electrochemical data of the compounds **1**, **5**, and **6**. Optical measurements were performed in $CHCl_3$; electrochemical measurements were performed in THF.

	λ_{abs} [nm] (ε [M^{-1} cm^{-1}])	λ_{onset} [nm][a]	λ_{ex} [nm]	λ_{em} [nm][b]	Φ_{PL} [%][c]	Stokes shift [cm^{-1}][d]	E_{HOMO}/E_{LUMO} [eV][e]	$E_{1/2}$ [V]	E_G^{opt} [eV][f]
1	266 (22800) 274 (27500) 366 (6200) 383 (10000) 402 (8700)	413	383	415 436 470 (sh)	39	779	–5.48/–2.48	–2.32	3.00
5	278 (25900) 286 (30600) 379 (11500) 396 (16300) 417 (12600)	435	397	441 462 500 (sh)	51 64[g] 54[h]	1334	–5.45/–2.60	–2.20	2.85
6	301 (sh) 318 (80000) 401 (sh) 431 (16200) 452 (12700)	477	318	481 506 559 (sh)	34 30[g] 50[i] 59[j]	1334	–5.40/–2.80	–2.00 –2.44	2.60

[a] Each onset wavelength (λ_{onset}) was determined by constructing a tangent on the point of inflection of the bathochromic slope of the most red-shifted absorption maximum. [b] Resolved vibrational fine-structure. [c] Quantum yields were determined by using a calibrated integrating sphere. [d] Stokes shifts represent the difference between each longest wavelength absorption maximum and the corresponding shortest wavelength emission maximum [e] $E_{HOMO} = E_{LUMO} - E_G^{opt}$, $E_{LUMO} = -4.8$ eV$-E_{1/2}^{Red1}$ (FcH/FcH$^+$ = –4.8 eV vs vacuum level). [f] Optical band gap $E_G^{opt} = 1240/\lambda_{onset}$. [g] Quantum yields measured in *c*-hexane. [h] Quantum yields measured in THF. [i] Quantum yields measured in C_6H_6. [j] Quantum yields measured in C_6F_6; sh = shoulder.

6.1. UV/Vis absorption and emission spectra

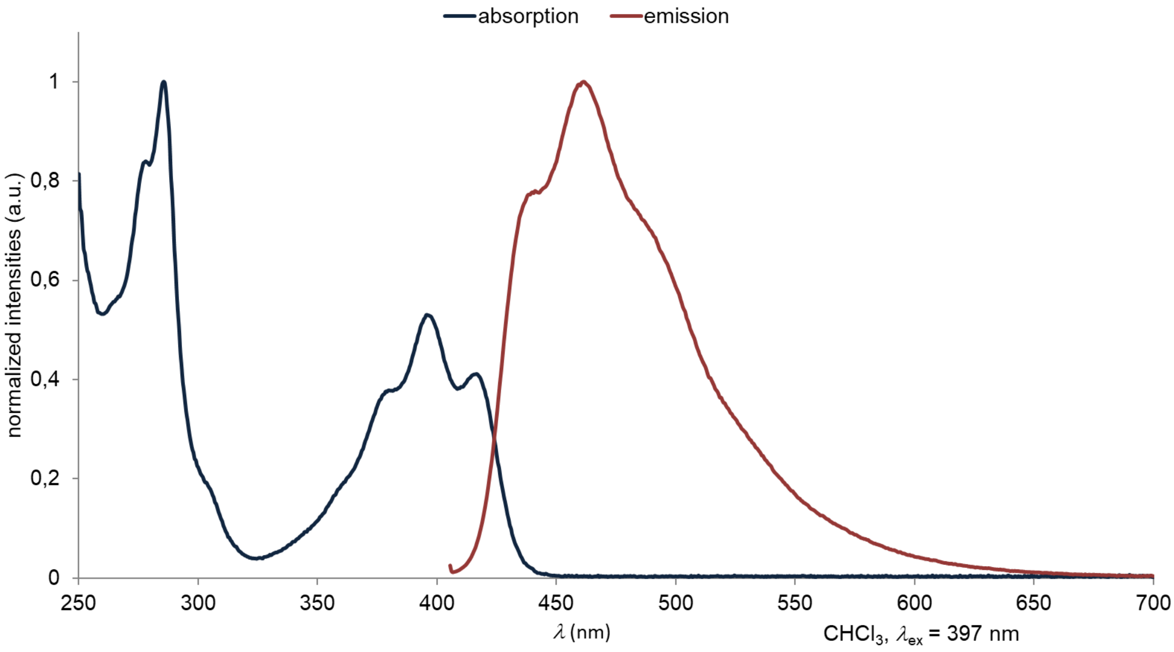

Figure S12: Normalized UV/Vis absorption and emission spectra of **5** in $CHCl_3$.

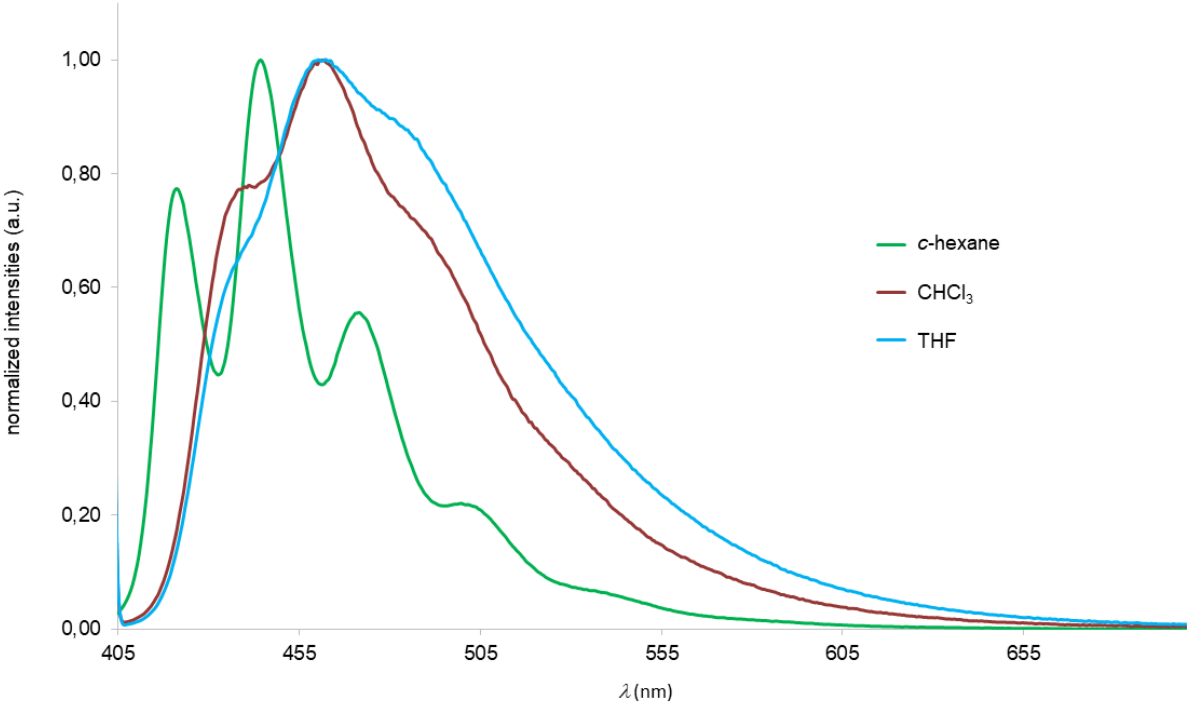

Figure S13: Normalized emission spectra of **5** in various solvents. In more polar solvents, the emission maximum is shifted to lower energy due to stabilization of the excited state, which typically has a larger dipole moment than the ground state.[S8]

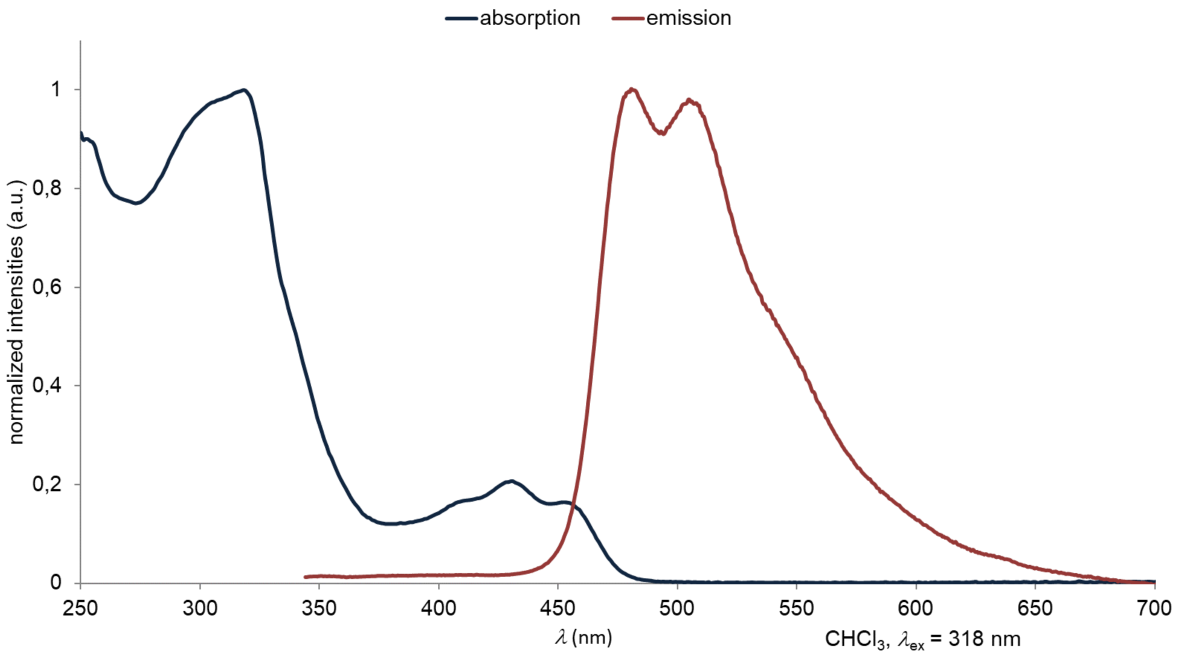

Figure S14: Normalized UV/Vis absorption and emission spectra of **6** in $CHCl_3$.

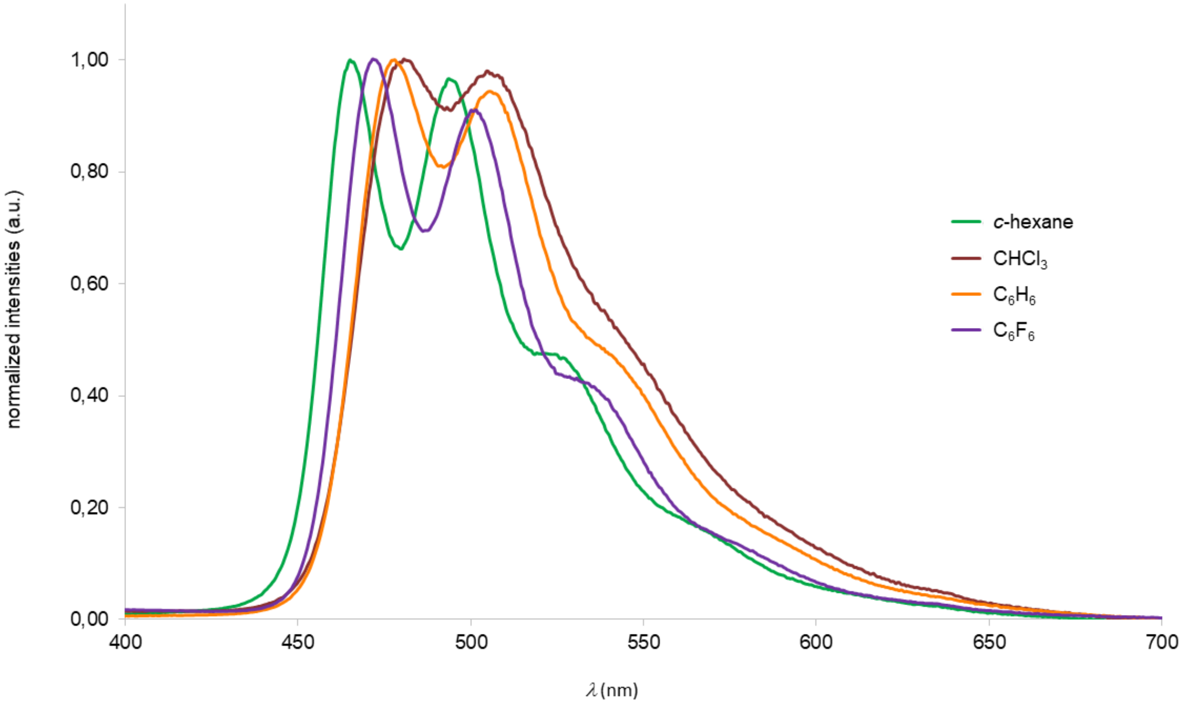

Figure S15: Normalized emission spectra of **6** in various solvents. In more polar solvents, the emission maximum is shifted to lower energy due to stabilization of the excited state, which typically has a larger dipole moment than the ground state.[S8]

6.2. Plots of cyclic voltammograms

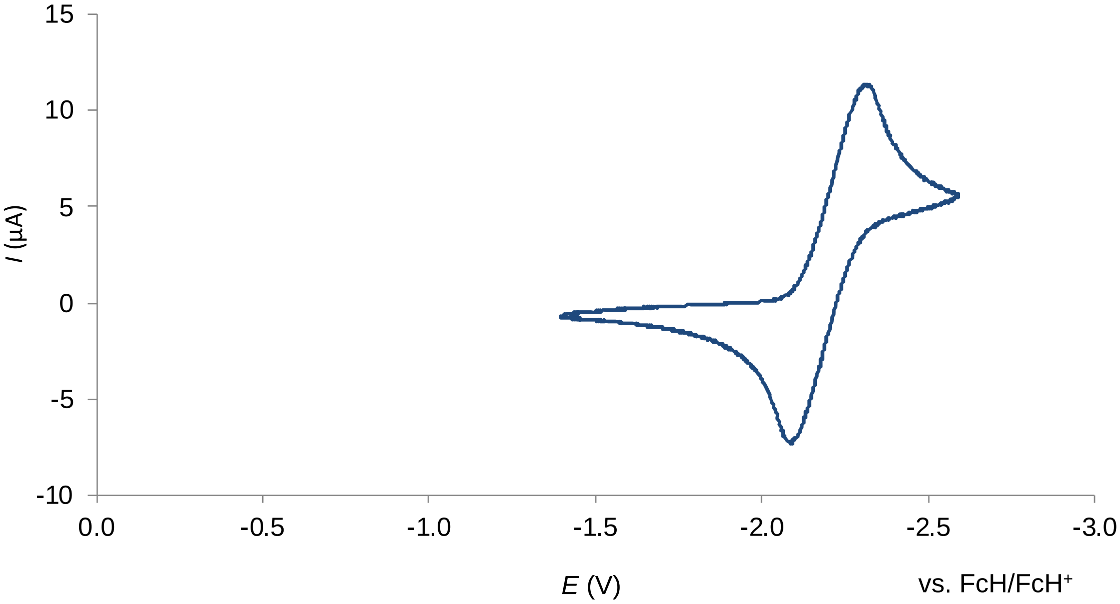

Figure S16: Cyclic voltammogram of **5** in THF (cathodic scan; room temperature, supporting electrolyte: [nBu$_4$N][PF$_6$] (0.1 M), scan rate 200 mV s^{-1}).

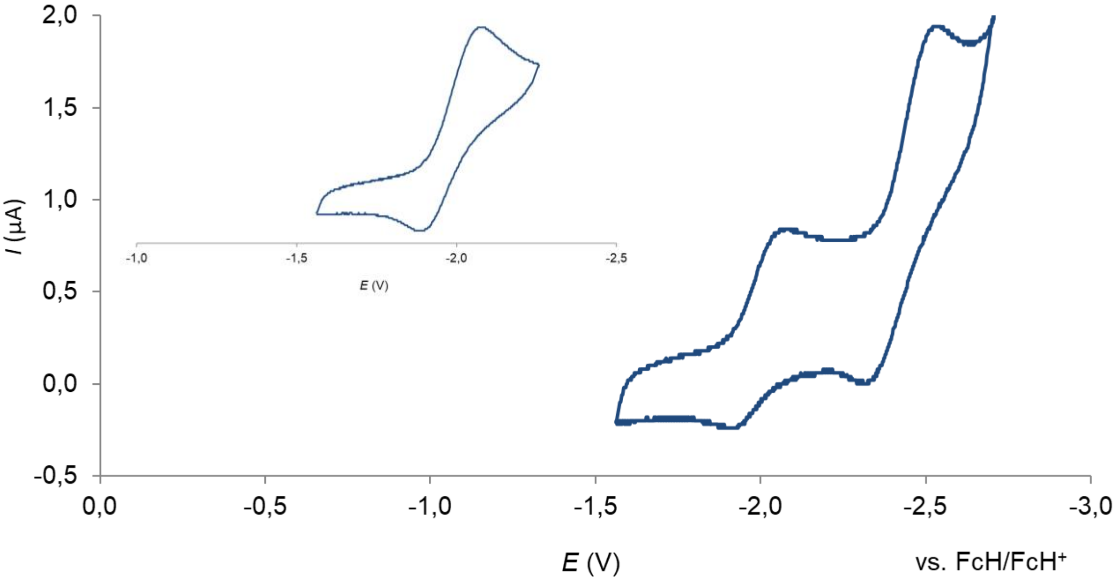

Figure S17: Cyclic voltammogram of **6** in THF (cathodic scan; room temperature, supporting electrolyte: [nBu$_4$N][PF$_6$] (0.1 M), scan rate 200 mV s^{-1}). Insert: First redox wave only with a switching potential of −2.26 V.

7. X-ray crystal structure analyses

Data for all structures were collected on a STOE IPDS II two-circle diffractometer with a Genix Microfocus tube with mirror optics using MoK_α radiation (λ = 0.71073 Å) and were scaled using the frame-scaling procedure in the *X-AREA*[S9] program system. The structures were solved by direct methods using the program *SHELXS*[S10] or *SHELXT*[S10] and refined against F^2 with full-matrix least-squares techniques using the program *SHELXL-97*[S10] or *SHELXL-2018/3*.[S10]

In the structure of **2** (CCDC 2191244), the contribution of the solvent was suppressed using the *SQUEEZE* routine in *PLATON*.[S11] The cavity volume (144 Å^3), the number of electrons (38) and the residual density map are in good agreement with one crystallographically unique THF molecule severely disordered around the inversion point of the $R-3$ space group. Therefore, the chemical formula of the crystal used for SC-XRD is **2**•0.33THF. The planar molecule (r.m.s. deviation for all non-H atoms: 0.008 Å) is located on a center of inversion. The molecules form skew stacks in the crystal lattice with an interplanar distance of 3.47 Å. The offset between the centroids of two molecules is 1.82 Å.

The single crystal of **3** (CCDC 2191247) used for the SC-XRD is a solid solution of **3** and **2** with the composition $(\mathbf{3})_{0.865}(\mathbf{2})_{0.135}$. As a result, the terminal Br atom at the CH_2 group occupies its position by 86.5%. Because of the presence of the inversion center, the co-crystallization of a triply brominated species possessing the core of compound **2** and bearing one CH_2Br and one CH_3 group would also be conceivable. However, this less symmetric compound would be expected to have higher solubility than both **2** and **3**. The molecule of **3** is located on a center of inversion, and the molecule is planar (r.m.s. deviation for all non-H atoms: 0.022Å). The crystal packing shows a herringbone pattern. The molecules form skew stacks in the crystal lattice with an interplanar distance of 3.40 Å. The offset between the centroids of two molecules is 3.51 Å

Compound **4** (CCDC 2191246) crystallizes as twofold twins of triclinic individuals related by rotation about [100]. Intensity data of both domains were integrated concurrently with overlap information (HKLF5). The refined twin volume ratio was 65.9:34.1(2). The molecule is located on a center of inversion. The B_2,O_2-perylene moiety is planar (r.m.s. deviation for all non-H atoms: 0.030 Å). The bromine atom Br(1) and the methyl-C atom C(9) deviate only slightly from this plane (0.002 Å for Br(1) and 0.043 Å for C(9)), whereas the bromine atom Br(2) is displaced by 0.123 Å. The molecules form skew stacks in the crystal lattice with an interplanar distance of 3.44 Å. The offset between the centroids of two molecules is about 2.18 Å.

The crystals of **5** (CCDC 2191245) scatter very weakly. Even long exposure (6 min / 1 deg frame) did not allow to obtain good high-angle data. After careful analysis of the I_{hkl}/σ *vs* resolution table, we decided to discard all reflections above d_{min} = 0.95 Å ($sin\Theta/\lambda$ = 0.526 Å^{-1}). The molecule is located on a center of inversion. The B_2,O_2-perylene moiety is planar (r.m.s. deviation for all non-H atoms: 0.010 Å). The crystal packing shows a herringbone pattern. The molecules form skew stacks with an interplanar distance of 3.53 Å. The offset between the centroids of two molecules is 2.24 Å.

Compound **6** (CCDC 2191248) crystallizes with two molecules and four molecules of C_6H_6 in the asymmetric unit. Four *t*Bu groups are disordered over two positions with site occupation factors of 0.588(9), 0.531(13), 0.756(11), and 0.686(10) for the major occupied sites. The displacement parameters of the disordered atoms were restrained to an isotropic behavior. The bond distances in one benzene molecule were restrained to 1.40(1)Å. The B_2,O_2-perylene moieties are essentially planar (r.m.s. deviation for non-H atoms: 0.024Å and 0.027Å for the two molecules in the asymmetric unit). The molecules form skew stacks in the crystal lattice with the sequence AABBAABB. The interplanar distances between the B_2,O_2-perylene moieties are 3.54 Å (AA), 3.49 Å (AB), 3.56 Å (BB). The offsets between the centroids of the perylene moieties of two molecules are 5.59 Å (AA), 3.82 Å (AB), 4.60 Å (BB).

CCDC files **2**-**6** (2191244–2191248) contain the supplementary crystallographic data for this paper and can be obtained free of charge from The Cambridge Crystallographic Data Centre via www.ccdc.cam.ac.uk/data_request/cif.

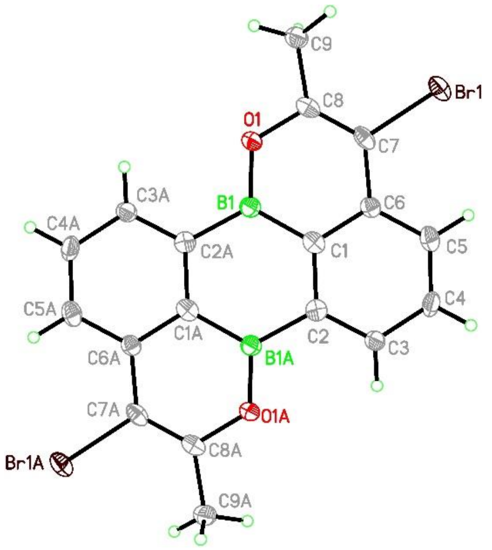

Figure S18 (CCDC 2191244): Molecular structure of **2** in the solid state. Displacement ellipsoids are drawn at the 50% probability level. Selected bond lengths (Å), bond angles (°), and torsion angles (°): B(1)–O(1) = 1.388(6), O(1)–C(8) = 1.378(6), C(7)–C(8) = 1.350(7), Br(1)–C(7) = 1.902(5); O(1)–B(1)–C(1) = 117.9(4), O(1)–B(1)–C(2A) = 119.7(4), C(1)–B(1)–C(2A) = 122.5(4), C(7)–C(8)–C(9) = 127.8(5), Br(1)–C(7)–C(8) = 118.2(4); O(1)–B(1)–C(1)–C(6) = 1.7(6), C(2)–C(1)–C(6)–C(7) = 179.6(4), Br(1)–C(7)–C(8)–C(9) = −0.6(6). Symmetry transformation used to generate equivalent atoms: −x+1/3, −y+2/3, −z+2/3.

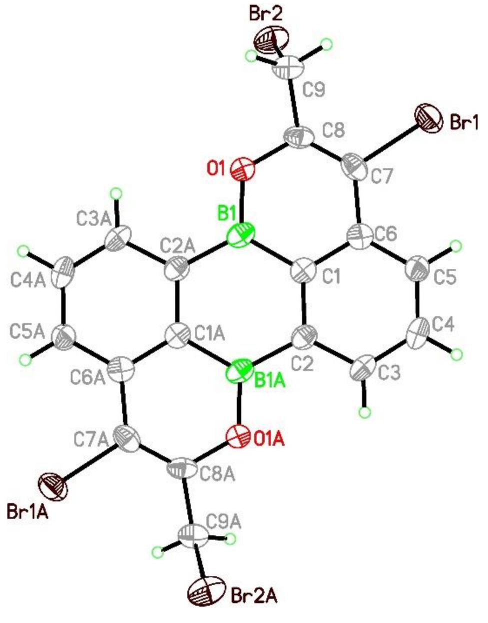

Figure S19 (CCDC 2191247): The single crystal of **3** used for the SC-XRD is a solid solution of **3** and **2** with the composition (**3**)$_{0.865}$(**2**)$_{0.135}$. Molecular structure of **3** in the solid state. Displacement ellipsoids are drawn at the 50% probability level. Selected bond lengths (Å), bond angles (°), and torsion angles (°): B(1)–O(1) = 1.386(8), O(1)–C(8) = 1.374(7), C(7)–C(8) = 1.339(12), Br(1)–C(7) = 1.890(6), Br(2)–C(9) = 1.933(7); O(1)–B(1)–C(1) = 118.2(5), O(1)–B(1)–C(2A) = 119.5(5), C(1)–B(1)–C(2A) = 122.3(5), C(7)–C(8)–C(9) = 127.3(6), Br(1)–C(7)–C(8) = 118.4(5); O(1)–B(1)–C(1)–C(6) = 0.6(8), C(2)–C(1)–C(6)–C(7) = −178.2(5), Br(1)–C(7)–C(8)–C(9) = −2.6(9), Br(2)–C(9)–C(8)–O(1) = −84.1(6). Symmetry transformation used to generate equivalent atoms: −x+1, −y+1, −z+1.

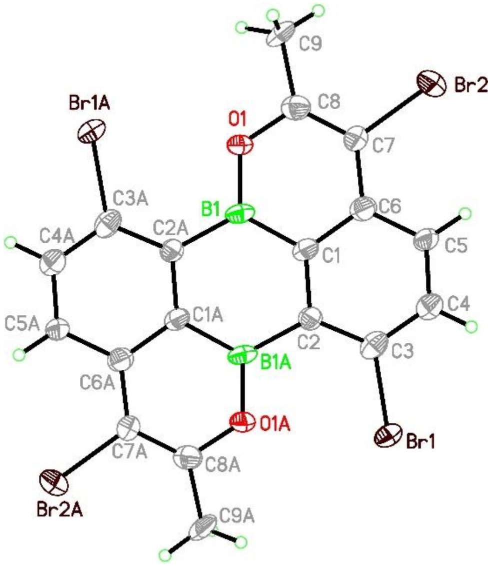

Figure S20 (CCDC 2191246): Molecular structure of **4** in the solid state. Displacement ellipsoids are drawn at the 50% probability level. Selected bond lengths (Å), bond angles (°), and torsion angles (°): B(1)–O(1) = 1.386(15), O(1)–C(8) = 1.372(14), C(7)–C(8) = 1.351(17), Br(1)–C(3) = 1.905(12), Br(2)–C(7) = 1.894(13); O(1)–B(1)–C(1) = 117.3(11), O(1)–B(1)–C(2A) = 119.1(11), C(1)–B(1)–C(2A) = 123.6(10), C(7)–C(8)–C(9) = 128.2(11), Br(2)–C(7)–C(8) = 118.0(9), Br(1)–C(3)–C(2) = 122.9(9); O(1)–B(1)–C(1)–C(6) = −1.4(16), C(2)–C(1)–C(6)–C(7) = 179.4(11), Br(2)–C(7)–C(8)–C(9) = −2.9(18), Br(1)–C(3)–C(2)–B(1A) = 0.6(18). Symmetry transformation used to generate equivalent atoms: −x+2, −y, −z+1.

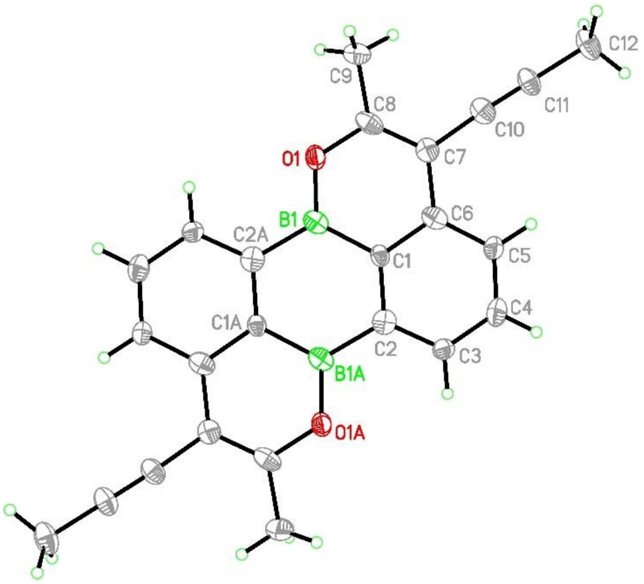

Figure S21 (CCDC 2191245): Molecular structure of **5** in the solid state. Displacement ellipsoids are drawn at the 50% probability level. Selected bond lengths (Å), bond angles (°), and torsion angles (°): B(1)–O(1) = 1.385(8), O(1)–C(8) = 1.376(7), C(7)–C(8) = 1.351(8), C(10)–C(11) = 1.185(8); O(1)–B(1)–C(1) = 117.8(5), O(1)–B(1)–C(2A) = 119.6(5), C(1)–B(1)–C(2A) = 122.6(5), C(7)–C(8)–C(9) = 125.8(5), C(8)–C(7)–C(10) = 119.8(6), C(7)–C(10)–C(11) = 177.3(8); O(1)–B(1)–C(1)–C(6) = 1.2(7), C(2)–C(1)–C(6)–C(7) = 179.6(6), C(10)–C(7)–C(8)–C(9) = −1.0(9). Symmetry transformation used to generate equivalent atoms: −x+1, −y, −z+1.

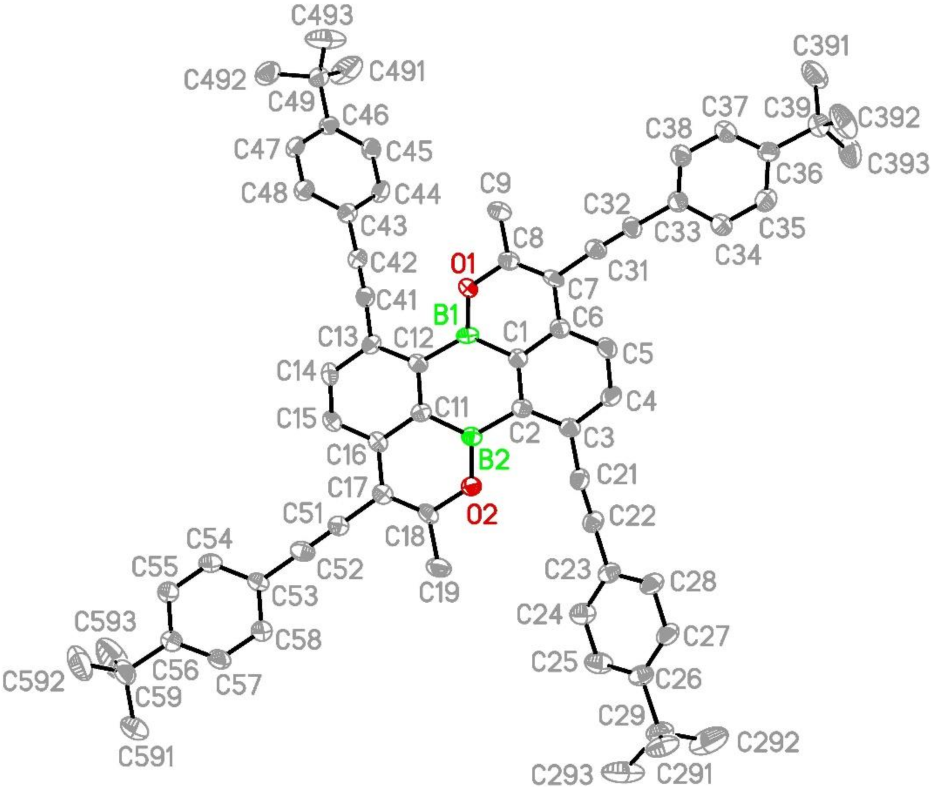

Figure S22 (CCDC 2191248): Compound **6** crystallizes with two crystallographically independent molecules in the asymmetric unit (**6A**, **6B**). Molecular structure of **6A** in the solid state. Displacement ellipsoids are drawn at the 50% probability level. Selected bond lengths (Å), bond angles (°), and torsion angles (°): B(1)–O(1) = 1.381(5), B(2)–O(2) = 1.384(6), O(1)–C(8) = 1.354(5), O(2)–C(18) = 1.367(5), C(7)–C(8) = 1.351(6), C(17)–C(18) = 1.353(6), C(21)–C(22) = 1.202(6), C(31)–C(32) = 1.180(6), C(41)–C(42) = 1.195(6), C(51)–C(52) = 1.174(6); O(1)–B(1)–C(1) = 117.1(4), O(1)–B(1)–C(12) = 119.3(4), C(1)–B(1)–C(12) = 123.6(4), O(2)–B(2)–C(2) = 119.3(4), O(2)–B(2)–C(11) = 117.2(4), C(2)–B(2)–C(11) = 123.5(4), C(3)–C(21)–C(22) = 173.2(5), C(7)–C(31)–C(32) = 176.5(5), C(13)–C(41)–C(42) = 175.8(5), C(17)–C(51)–C(52) = 179.3(5); O(1)–B(1)–C(1)–C(6) = 0.3(5), O(2)–B(2)–C(11)–C(16) = 0.8(5), C(2)–C(1)–C(6)–C(7) = 178.7(4), C(2)–C(1)–C(6)–C(7) = 178.2(4), C(31)–C(7)–C(8)–C(9) = −2.4(7), C(51)–C(17)–C(18)–C(19) = −1.8(7).

Table S2: Selected crystallographic data for **2 – 4.**

compound	**2**	**3**	**4**
CCDC	2191244	2191247	2191246
formula	$C_{18}H_{12}B_2Br_2O_2\cdot$ $0.33(C_4H_8O)$	$0.865(C_{18}H_{10}B_2Br_4O_2)\cdot$ $0.135(C_{14}H_{12}B_2Br_2O_2)$	$C_{18}H_{10}B_2Br_4O_2$
M_r	465.75	578.52	599.52
T (K)	173(2)	173(2)	173(2)
radiation, λ (Å)	0.71073	0.71073	0.71073
crystal system	trigonal	monoclinic	triclinic
space group	$R-3$	$P\,2_1/c$	$P-1$
a [Å]	33.594(3)	13.9949(14)	4.0696(5)
b [Å]	33.594(3)	4.1803(3)	10.3082(15)
c [Å]	3.9159(5)	15.8146(15)	11.2049(15)
α [°]	90	90	70.3780(11)
β [°]	90	106.946(7)	89.574(10)
γ [°]	120	90	80.955(11)
V [Å^3]	3827.2(8)	885.03(14)	436.73(10)
Z	9	2	1
D_{calcd} (g cm^{-3})	1.819	2.170	2.280
μ (mm^{-1})	4.779	8.495	9.226
F(000)	2064	550	284
crystal size (mm^3)	0.210 × 0.080 × 0.080	0.130 × 0.010 × 0.010	0.120 × 0.030 × 0.020
Θ [°]	4.203 to 25.587	3.426 to 25.629	2.126 to 25.522
h	−40 to 40	−13 to 17	−4 to 4
k	−40 to 33	−5 to 5	−12 to 12
l	−4 to 4	−19 to 19	−13 to 13
reflections collected	3567	5747	9175
independent reflections	1584	1637	9175
R_{int}	0.0481	0.0398	Not determined due to twinning
data/restraints/parameters	1584/0/110	1637/0/120	9175/0/120
R_1, wR_2 (I > 2σ(I))	0.0446, 0.0916	0.0449, 0.0980	0.0631, 0.1406
R_1, wR_2 (all data)	0.0634, 0.0978	0.0601, 0.1046	0.1031, 0.1666
Goodness-of-fit on F^2	1.033	1.081	1.034
largest diff. peak and hole (e Å^{-3})	0.737 and −0.447	0.628 and −0.668	0.542 and −0.720

Table S3: Selected crystallographic data for **5** and **6**.

compound	**5**	**6**
CCDC	2191245	2191248
formula	$C_{24}H_{18}B_2O_2$	$C_{66}H_{62}B_2O_2 \cdot 2(C_6H_6)$
M_r	360.00	1064.99
T (K)	173(2)	173(2)
radiation, λ (Å)	0.71073	0.71073
crystal system	monoclinic	triclinic
space group	$P\,2/n$	$P\,-1$
a [Å]	10.1295(16)	17.119(2)
b [Å]	4.8835(8)	19.603(2)
c [Å]	18.636(3)	21.410(2)
α [°]	90	103.695(9)
β [°]	102.228(13)	112.951(10)
γ [°]	90	95.721(10)
V [Å^3]	901.0(3)	6278.3(14)
Z	2	4
D_{calcd} (g cm^{-3})	1.327	1.127
μ (mm^{-1})	0.081	0.065
F(000)	376	2272
crystal size (mm^3)	0.190 × 0.070 × 0.030	0.270 × 0.240 × 0.120
Θ [°]	3.546 to 21.963	3.348 to 25.027
h	−10 to 10	−20 to 20
k	−5 to 5	−23 to 22
l	−19 to 19	−25 to 25
reflections collected	2899	62154
independent reflections	1096	22097
R_{int}	0.0936	0.0633
data/restraints/parameters	1096/0/129	22097/150/1593
R_1, wR_2 ($I > 2\sigma(I)$)	0.0792, 0.1138	0.1114, 0.1909
R_1, wR_2 (all data)	0.1653, 0.1361	0.1898, 0.2194
Goodness-of-fit on F^2	1.013	1.159
largest diff. peak and hole (e Å^{-3})	0.187 and −0.234	0.446 and −0.208

8. References

S1 J.-F. Betzer, J. Ardisson and A. Pancrazi, *C. R. Acad. Sci. Paris, Chemistry*, 2001, **4**, 695–704.

S2 W. Senevirathna, J. Liao, Z. Mao, J. Gu, M. Porter, C. Wang, R. Fernando and G. Sauvé, *J. Mater. Chem. A*, 2015, **3**, 4203–4214.

S3 T. Kaehler, M. Bolte, H. W. Lerner and M. Wagner, *Angew. Chem. Int. Ed.*, 2019, **58**, 11379–11384.

S4 G. R. Fulmer, A. J. M. Miller, N. H. Sherden, H. E. Gottlieb, A. Nudelman, B. M. Stoltz, J. E. Bercaw and K. I. Goldberg, *Organometallics*, 2010, **29**, 2176–2179.

S5 K. Suzuki, A. Kobayashi, S. Kaneko, K. Takehira, T. Yoshihara, H. Ishida, Y. Shiina, S. Oishi and S. Tobita, *Phys. Chem. Chem. Phys.*, 2009, **11**, 9850–9860.

S6 A. M. Brouwer, *Pure Appl. Chem.*, 2011, **83**, 2213–2228.

S7 T.-S. Ahn, R. O. Al-Kaysi, A. M. Müller, K. M. Wentz and C. J. Bardeen, *Rev. Sci. Instrum.*, 2007, **78**, 086105.

S8 J. R. Lakowicz, *Principles of Fluorescence Spectroscopy*, Springer US, New York, 3rd edn., 2006.

S9 Stoe & Cie, *X-AREA*. *Diffractometer control program system*. Stoe & Cie, Darmstadt, Germany, 2002.

S10 G. M. Sheldrick, *Acta Crystallogr. A*, 2008, **64**, 112–122.

S11 A. L. Spek, *Acta Crystallogr. D*, 2009, **65**, 148–155.